

## Measurement of Low Light Intensities by Synchronous Single Photon Counting\*†

F. T. ARECCHI, E. GATTI,‡ AND A. SONA

Laboratori C.I.S.E., Segrate, Milano, Italy

(Received 29 November 1965; and in final form, 4 March 1966)

Single photon counting technique is used for measuring continuous light fluxes of very low intensity suitably modulated. Demodulation and integration processes usually made in conventional synchronous detectors on analog signals are here performed with drift free digital operations. The main advantage of this procedure is the possibility of improving the signal-to-noise ratio by very long integration times which are not limited by drifts of the electronics following the detector. An analysis of the noise filtering properties of the device is given. Raman light angular distributions obtained by this technique are reported as an example and noise characteristics of the device are measured and compared with the results of the theoretical analysis.

### 1. INTRODUCTION

IN some optical experiments (for instance Raman or Brillouin scattering or harmonic generation) resolution both in angle and in frequency is limited by the requirement of a sufficient amount of input light in the measuring device, in order to obtain a good signal-to-noise ratio. The problem occurs more generally in any spectroscopic investigation, from low frequency to the optical range, and is usually solved either by frequency domain filtering, i.e., narrowband detectors, in connection with modulation and demodulation systems (synchronous detectors) or time domain filtering accomplished for instance by averaging techniques.

In the optical range a single photon can release a sizeable amount of charge at the output of a photomultiplier and, at low light intensities, contributions from single photoelectrons are resolved in time, so that the signal can be extracted in a digital form by counting techniques. We have exploited this possibility in a device which performs the operations of demodulation and time averaging by digital techniques.

### 2. SYNCHRONOUS SINGLE PHOTON COUNTING DETECTOR

The block diagram of our synchronous single photon counting (SSPC) detector used in a low intensity light flux measurements is shown in Fig. 1. Excitation source ES can be either a light source (as in a Raman or Brillouin scattering experiment) or any other source which, interacting with cell C, gives rise to the low intensity light flux L at the input of the detector PM. This flux is modulated either closing periodically the optical path from C to PM or interrupting periodically the interaction between the

excitation source and the cell. Detector PM is a high gain photomultiplier with a single electron response (SER) suitable to drive a standard pulse shaper circuit at its output which triggers for pulses above a set threshold level A. (For instance, photomultipliers Philips 56 AVP, as well as RCA 7265 can be used for this purpose). An electronic gate with a standard duration  $\tau$  is opened synchronously with the chopper by means of a suitable driving signal (derived from photodiode P looking at source S through the chopper wheel). An electronic switch actuated synchronously with the chopper sends the pulses coming out from the gate to the "add" or "subtract" input of a bidirectional counter (BC). The complete timing chart is shown in Fig. 2. Note that the "add" and "subtract" intervals are made equal by the same timing device actuating the electronic gate.

The operation of the system can be described as follows. During the "open" time of the chopper the photomultiplier output consists of signal pulses with average rate  $f_s(A)$  due to the emitted photoelectrons and of noise pulses with average rate  $f_n(A)$  coming from thermal electrons emitted either by photocathode or by other electrodes (dark current). All of them are sent to the "add" input of the BC. During the "close" time of the chopper only noise pulses are present and they are sent to the "subtract" input of the BC. The output of the BC is the average number of signal pulses. After a measuring time  $T$  the average reading of the BC is

$$S = f_s \eta T, \quad (1)$$

where  $\eta = \tau/t_0$  is the ratio of the two equal counting intervals  $\tau$ , alternatively used for the add and the subtract operations, to the chopper period  $t_0$  ( $\eta \leq \frac{1}{2}$ ).

The rms deviation  $\epsilon_n$  of the BC reading is given by

$$\epsilon_n = [(2f_n + f_s)\eta T]^{\frac{1}{2}}, \quad (2)$$

and therefore the signal-to-noise ratio is

$$S/\epsilon_n = f_s(\eta T)^{\frac{1}{2}}/(2f_n + f_s)^{\frac{1}{2}}. \quad (3)$$

With no input signal the counter reading is in average zero, its position is affected by noise which gives rise to a

\* Work partially supported by the C.N.R. (Italian National Research Council).

† After this work was completed T. A. Kovaleva, A. E. Melamid, A. N. Pisarevskii, I. V. Reznikov, and S. S. Shushkevich, "Method of Statistical Recording of Luminescence Spectra at the Single Electron Level" appeared in *Pribery i Tekhn. Eksperim.* 2, 150 (1965) [English transl.: *Instr. Exptl. Tech.* (USSR) 2, 398 (1965)]. The device shown there is based on the same principle as ours.

‡ Istituto di Fisica del Politecnico, Milano, Italy, and C.I.S.E.

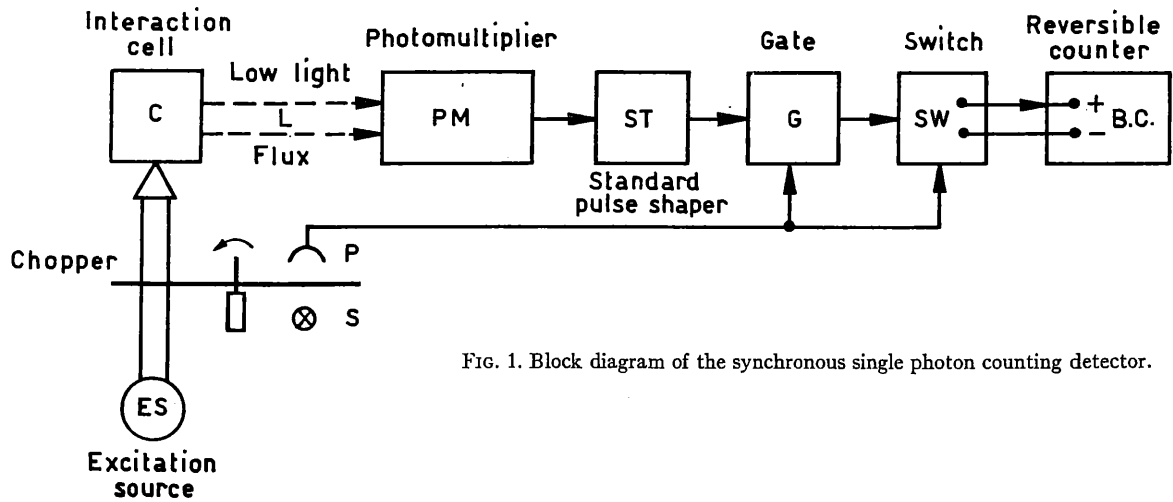


FIG. 1. Block diagram of the synchronous single photon counting detector.

“random walk” in the counter reading with a rms deviation  $\epsilon_n$ .

Apart from the procedure of continuously alternating signal and noise measurements to reduce drift and fluctuation effects, our system is equivalent to a flux counting procedure as used in nuclear physics, where two successive measurements of flux plus background alone are made for equal time intervals. It is well-known that this is the best subdivision of the measuring time when the background rate is much larger than the signal rate ( $f_n \gg f_s$ ).

### 3. NOISE FILTERING PROPERTIES AND THRESHOLD OPTIMIZATION

Further contribution to the noise due to the statistical average performed by the BC [see Eq. (2)] can arise from fluctuations in the average rate both of signal and noise pulses. Moreover any fluctuation in the analog elements of the detection chain, such as the threshold level  $A$  of the pulse shaper or the sampling time  $\tau$ , results in a fluctuation both in the signal and noise average pulse rate.

Assume that the average signal rate  $f_s$  is affected by

some perturbation  $s(t)$ , with power spectrum  $s(\omega)$ , so that  $f_s(t) = f_{s0}[1 + s(t)]$ . Due to the modulation and demodulation processes the signal pulse rate at the counter input is given by (notation of Woodward<sup>1</sup> is used as reported in the Appendix)

$$f_s^+(t) = f_s(t) \text{ rep}_{\nu_0} \text{ rect}(t/\tau),$$

(where  $\nu_0 = 1/t_0$  is the chopping frequency) and the associated power spectrum is

$$f_{s0}^2 [\eta^2 \text{ comb}_{\nu_0} \text{ sinc}^2(\omega\tau/2\pi) + s^+(\omega)],$$

where

$$s^+(\omega) = \eta^2 [s(\omega) + s(\omega - 2\pi\nu_0) \text{ sinc}^2\eta + s(\omega - 4\pi\nu_0) \text{ sinc}^2 2\eta + \dots]. \quad (4)$$

The number of signal pulses expected in the measuring interval is

$$S = \int_t^{t+T} f_s^+(t) dt;$$

an analysis of its statistical properties leads to the following expression for the variance of the accumulated signal counts, in terms of the ensemble average  $\bar{S}$  and variance  $\epsilon_s^2$  of  $S$ ,

$$\epsilon_s^2 = \epsilon_s^2 + \bar{S}. \quad (5)$$

Assume that the average noise pulse rate  $f_n$  is affected by some perturbation  $n(t)$  with power spectrum  $n(\omega)$  so that  $f_n = f_{n0}[1 + n(t)]$ . Due to the demodulation process the actual noise pulse rate at the add input of the BC is given by

$$f_{n1}^+(t) = f_{n0}[1 + n(t)] \text{ rep}_{\nu_0} \text{ rect}(t/\tau).$$

The number of noise pulses expected at the add input in

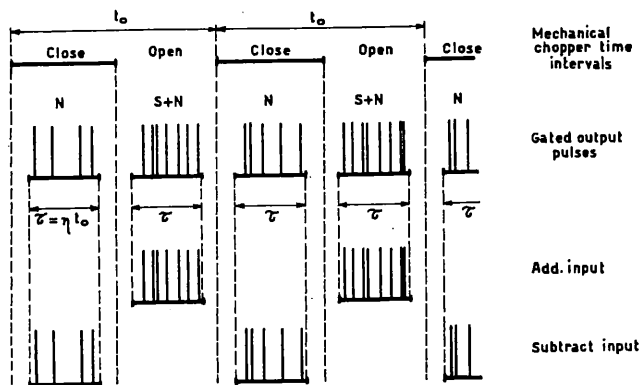


FIG. 2. Timing chart of the SSPC detector.

<sup>1</sup> P. M. Woodward, *Probability and Information Theory with Applications to Radar* (Pergamon Press, Inc., London, 1953), pp. 28-30.

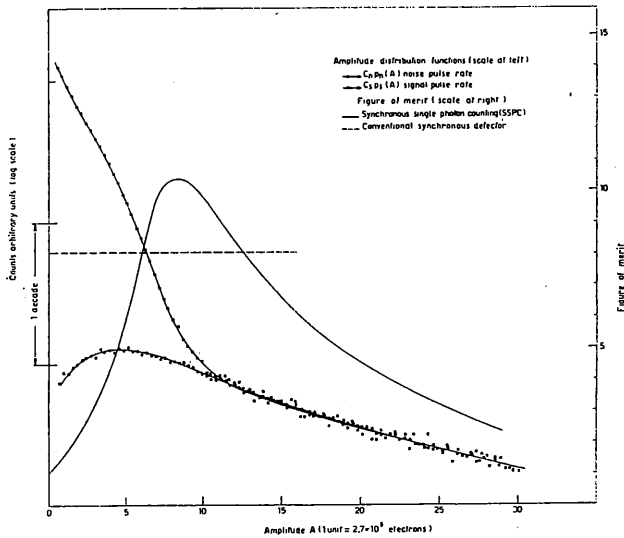


FIG. 3. Amplitude distribution functions of signal and noise pulse rates for a 56 AVP multiplier phototube at room temperature. The figure of merit of the SSPC system versus threshold amplitude  $A$  is also plotted and compared with the one obtainable with a conventional synchronous detection system.

the interval  $(t, t+T)$  is

$$N_1 = \int_t^{t+T} f_{n1}^+(t) dt,$$

with an ensemble average  $\bar{N}_1$ . Similarly the noise pulse rate at the BC subtract input is

$$f_{n2}^+(t) = f_{n0}[1+n(t)] \text{rep}_{\nu_0} \text{rect}[(t-t_0/2)/\tau].$$

The number of noise pulses expected at the subtract input in the interval  $(t, t+T)$  is given by

$$N_2 = \int_t^{t+T} f_{n2}^+(t) dt,$$

with an average  $\bar{N}_2$ . The power spectrum of  $f_{n1}^+(t) - f_{n2}^+(t)$  is given by

$$f_{n0}[\eta^2 \text{comb}_{\nu_0} \text{sinc}^2(\omega\tau/2\pi) 2(1 - \frac{1}{2} \cos\omega t_0) + n^+(\omega)],$$

where

$$n^+(\omega) = 4\eta^2 [n(\omega - 2\pi\nu_0) \text{sinc}^2\eta + n(\omega - 6\pi\nu_0) \text{sinc}^2 3\eta + n(\omega - 10\pi\nu_0) \text{sinc}^2 5\eta + \dots]. \quad (6)$$

As for the signal it is easily shown that the variance of the accumulated noise counts is

$$\epsilon_2^2 = \epsilon_{N_1-N_2}^2 + \bar{N}_1 + \bar{N}_2, \quad (7)$$

where  $\epsilon_{N_1-N_2}$  is the variance of  $N_1 - N_2$ . Variances  $\epsilon_s^2$  and  $\epsilon_{N_1-N_2}^2$  in Eqs. (5) and (7) are evaluated in terms of the signal and noise power spectra through the Wiener-Kintchine theorem; the final variance of the accumulated

counts in the time  $T$  is

$$\begin{aligned} \epsilon_{N^2} = \epsilon_1^2 + \epsilon_2^2 = & \bar{S} + 2f_{s0}^2 \int_0^\infty s^+(\omega) \frac{1 - \cos\omega T}{\omega^2} d\omega \\ & + \bar{N}_1 + \bar{N}_2 + 2f_{n0}^2 \int_0^\infty n^+(\omega) \frac{1 - \cos\omega T}{\omega^2} d\omega. \end{aligned}$$

If perturbations  $s(t)$  and  $n(t)$  have zero ensemble average this yields

$$\begin{aligned} \epsilon_{N^2} = & (f_{s0} + 2f_{n0})\eta T \\ & + 2 \int_0^\infty [f_{s0}^2 s^+(\omega) + f_{n0}^2 n^+(\omega)] \frac{1 - \cos\omega T}{\omega^2} d\omega. \quad (8) \end{aligned}$$

The first term is the statistical contribution typical of Poisson distributions. The second term is due to the signal and noise rate fluctuations and corresponds to the power spectra  $f_{s0}^2 s^+(\omega)$  and  $f_{n0}^2 n^+(\omega)$  filtered by the integration over a time  $T$ . The effect of this integration is that only the low frequency components of  $s^+(\omega)$  and  $n^+(\omega)$  in a bandwidth  $1/T$  are important. Taking into account Eqs. (4) and (6) one can conclude that substantial contributions to the integral in Eq. (8) are given only by low frequency components of  $s(\omega)$  and components of  $n(\omega)$  centered around  $2\pi\nu_0$ . This suggests orientative criteria for a proper selection of the chopper frequency  $\nu_0$  which has to be far from frequencies where  $n(\omega)$  has relatively high components (such as multiple of the line frequency or of the possible perturbing frequencies). Working at low intensities ( $f_{s0} < f_{n0}$ ) the noise statistical term is the most important. The next order contribution is due usually to  $s(\omega)$  which becomes important when

$$f_{s0}^2 \int_0^\infty s^+(\omega) \frac{1 - \cos\omega T}{\omega^2} d\omega > \eta f_{n0} T.$$

Signal-to-noise ratio is a function of the threshold level  $A$  of the standard pulse shaper connected to the PM. Let us denote by  $C_n p_n(A) = -df_n(A)/dA$  the amplitude distribution function of noise pulse rate,  $C_n$  being the total rate of noise pulses, and  $p_n(A)$  the associated normalized amplitude distribution function. Similarly let  $C_s p_s(A) = -df_s(A)/dA$  be the amplitude distribution function of signal pulse rate due to photoelectrons. Due to the contribution of dark current pulses not coming from the photocathode,  $p_n(A)$  differs from  $p_s(A)$  (see Bertolaccini and Cova<sup>2</sup> and Tusting *et al.*<sup>3</sup>). There is an optimum value  $A_m$  for the threshold level which can be easily determined by differentiating Eq. 3. When  $f_n(A) \gg f_s(A)$ , the maximum

<sup>2</sup> M. Bertolaccini and S. Cova, *Energia Nucl.* 10, 259 (1963).

<sup>3</sup> R. F. Tusting, Q. A. Kerns, and H. K. Knudsen, *IRE Trans. Nucl. Sci.* NS-9, No. 3, 118 (1962).

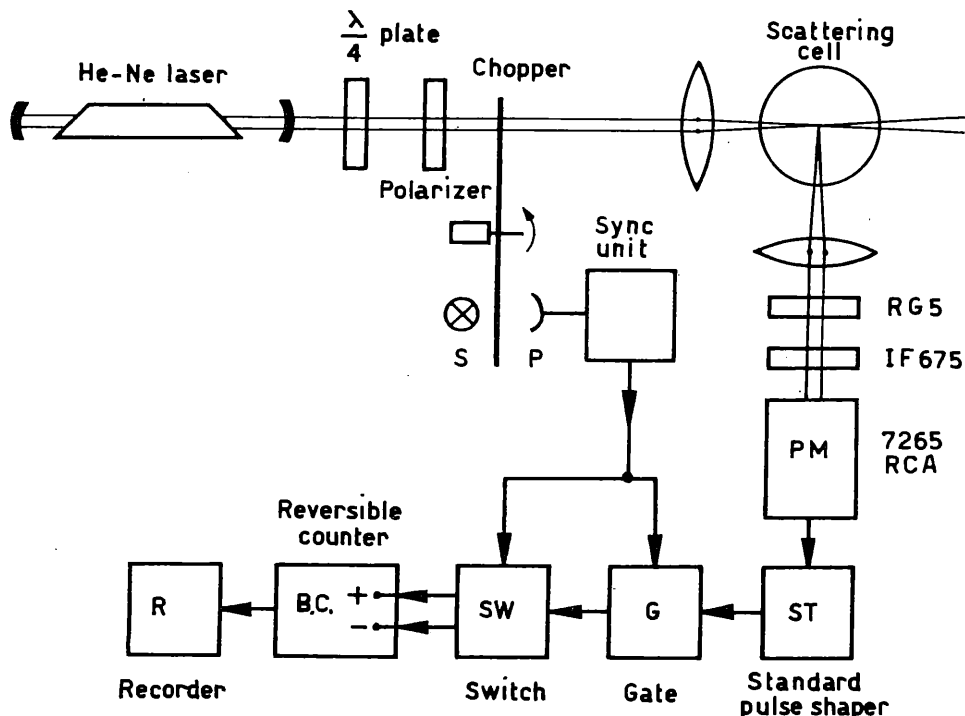


FIG. 4. Block diagram of the measurement of the Raman light angular distribution, with a He-Ne laser as the excitation source.

condition is

$$p_n(A) / \int_A^\infty p_n(A) dA = 2 \left[ p_s(A) / \int_A^\infty p_s(A) dA \right]. \quad (9)$$

The optimum value  $A_m$  which satisfies Eq. (9) depends only on the shape of the distributions  $p_s(A)$  and  $p_n(A)$ . The shape of  $p_n(A)$  is very sensitive to the operating conditions (photocathode temperature and operating voltage), therefore the optimum value of threshold  $A$  has to be determined experimentally by plotting  $f_s(A) / [2f_n(A)]^{1/2}$  at the operating conditions. As already observed, this optimization is significant only if, as usually happens, in the measuring time  $T$  the major contribution to the noise is given by the first term of Eq. (8). This threshold level optimization results in an improvement of the signal-to-noise ratio obtainable with SSPC which is peculiar to this counting technique. As an example Fig. 3 shows the amplitude distribution functions of signal and noise pulse rates  $-df_s(A)/dA$  and  $-df_n(A)/dA$  for a 56 AVP multiplier phototube, together with the figure of merit

$$(2/\eta T)(S^2/\epsilon_n^2)(C_n/C_s^2) = \int_A^\infty p_s(A) dA / \int_A^\infty p_n(A) dA,$$

as deduced from Eq. (3), vs threshold amplitude  $A$ . In the same figure, the horizontal line represents the figure of merit

$$(4/T)(S^2/\epsilon_n^2)(C_n/C_s^2) = \left[ \int_0^\infty A p_s(A) dA \right]^2 / \int_0^\infty A^2 p_n(A) dA,$$

which corresponds to a signal obtained by synchronous detection of the total phototube current followed by an integration for a time  $T$ . Such a device is taken as the model of the conventional synchronous detection system.

Further improvement of the SSPC technique could be obtained by adding a third channel. A monitor beam can be derived from the excitation source and sent to the photomultiplier through a three intervals chopper wheel. Pulses appearing at the photomultiplier output during the three time intervals correspond, respectively, to noise, signal plus noise, and monitor beam plus noise. Two BC and a three way switch are also required to have a measure of signal intensity and monitor beam intensity with automatic noise subtraction. Information on the monitor beam intensity takes into account all possible sources of drifts in the measuring chain, such as fluctuations of source intensity, threshold, gate time, and photomultiplier gain. The monitor signal can be used as a normalization parameter which can act automatically by stopping integration time at preset values of monitor signal counts.

#### 4. COMPARISON BETWEEN SSPC AND ANALOG SYNCHRONOUS DETECTORS

The main advantages of SSPC over analog synchronous detectors<sup>4,5</sup> (lock-in amplifiers) are due to the essentially drift free operations of the electronics following the photomultiplier and the standard pulse shaper. This allows

<sup>4</sup> R. Andrew, *Nuclear Magnetic Resonance* (University Press, Cambridge, England, 1965), p. 43-44.

<sup>5</sup> G. Feher, *Bell Syst. Techn. J.* 36, 480 (1957).

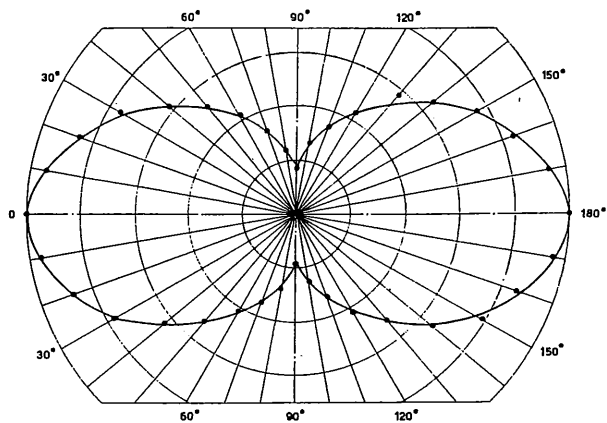


FIG. 5. Angular distribution of the  $992\text{ cm}^{-1}$  vibrational frequency of benzene obtained with SSPC detection technique.

very long integration times (of the order of hours) limited only by the stability of the preceding analog parts of the electronics.

As far as gate duration  $\tau$  is concerned, only short term stability is required (with respect to times of the order of several  $t_0$ ) due to the important feature of the SSPC that the time duration  $\tau$  of the gate during the "open" and "close" time of the chopper is determined by the same physical element. This allows an almost perfect demodulation process avoiding unbalance effects or nonlinear response.<sup>6</sup>

Threshold stability affects both signal and noise pulse rates; residual fluctuations can be corrected with additional monitoring techniques described in Sec. 3. All these fluctuation terms can be taken into account in the noise analysis of Sec. 3 inserting suitable components in the noise signal power spectra.

A disadvantage of our system is the need of a high gain photomultiplier in order to perform single photon counting while a lock-in amplifier can operate with any analog signal, moreover single photon counting technique has an upper limit for intensities due to the requirement of no appreciable counting losses. Its use is therefore restricted to low light intensities ( $<10^6$  photoelectrons/sec).

The principle of operation of the two types of detectors is quite similar: The main differences are digital demodulation and integration in the SSPC against analog demodulation and analog integration (i.e., bandwidth narrowing) in the lock-in amplifier. Noise filtering properties are also similar, apart from the larger integration time equivalent to a narrow bandwidth achievable with the SSPC and the additional improvement of the signal-to-noise ratio with threshold optimization. No phasing of the reference signal

<sup>6</sup> Automatic noise subtraction can be affected by an error due to deadtimes of the counting chain. They give a different contribution during the add and subtract periods, as the average counting rates are different due to the presence of signal pulses in the add channel. This effect is however of no importance in the more interesting case in which  $f_s \ll f_n$ .

is necessary as the gate time is precisely located inside the "open" and "close" chopper time intervals, to avoid errors due to mechanical imperfections of the chopper wheel.

The SSPC technique can be either applied with a single signal channel scheme or with a multichannel system to allow measurements on different signals (different wavelengths in a spectroscopic analysis for instance). In this case the operation in connection with an Enhancetron<sup>7,8</sup> seems to be very promising. A memory channel of the Enhancetron can be used to store noise pulses and another one to store signal pulses. If these two memory addresses are switched synchronously with the chopper, and noise automatic subtraction is then accomplished, the system performs the demodulation and integration processes in digital form. With this feature added a two channel Enhancetron behaves just as our system. A third memory cell can be used for the monitor signal while all other cells are available for storing pulses from different signals and performing automatic subtraction with a convenient scanning cycle.

## 5. EXPERIMENTAL RESULTS

A measurement of angular distribution of Raman light has been performed with the SSPC detector. The experimental setup is shown in Fig. 4. A laser beam is focused in the sample cell C filled with benzene and the Raman scattered light is observed at  $90^\circ$  with a 7265 RCA photomultiplier. The beam polarization can be rotated without changes in intensity by rotating the polarizer P inserted in the beam path after a  $\lambda/4$  plate. In Fig. 5 the angular distribution of the  $992\text{ cm}^{-1}$  vibrational frequency of benzene is reported for observation in a direction parallel to the polarization plane (see Damen *et al.*<sup>9</sup>). Photoelectron rates as low as 10 pulses/sec were measured after an integration time of 1 min in the presence of 500 noise pulses/sec, with a signal-to-noise ratio of 10. A 10 mW He-Ne laser at  $6328\text{ \AA}$  was used as an excitation source and the photomultiplier was operated at room temperature.

As a further test of the sensitivity and lack of drifts in the system a  $\frac{1}{2}$  h run of operation was recorded with a noise pulse frequency  $\eta f_n$  of 2700 pulses/sec and the "random walk" is contained within the limits of the statistical noise. This is a proof that analog drifts and average noise pulse rate fluctuations are unimportant at this noise level. A light signal giving a pulse rate  $\eta f_s = 10$  pulses/sec was then added and after a  $\frac{1}{2}$  h of measuring time it could be clearly detected with a signal-to-noise ratio of 6. Similar results are reported in Fig. 6 where several "random walks" are recorded with a noise pulse rate  $\eta f_n = 33.5$  pulses/sec with-

<sup>7</sup> M. K. Klein and G. W. Barton, Jr., *Rev. Sci. Instr.* **34**, 754 (1963).

<sup>8</sup> G. F. Mayers and R. T. Schneider "Spectroscopic Investigations of Plasma Properties," Quarterly summary Rept. No. 3, pp. 9-28, Contract No. NASw-992 EDR 4125 (1965).

<sup>9</sup> T. C. Damen, R. C. Leite, and S. P. S. Porto, *Phys. Rev. Letters* **14**, 9 (1965).

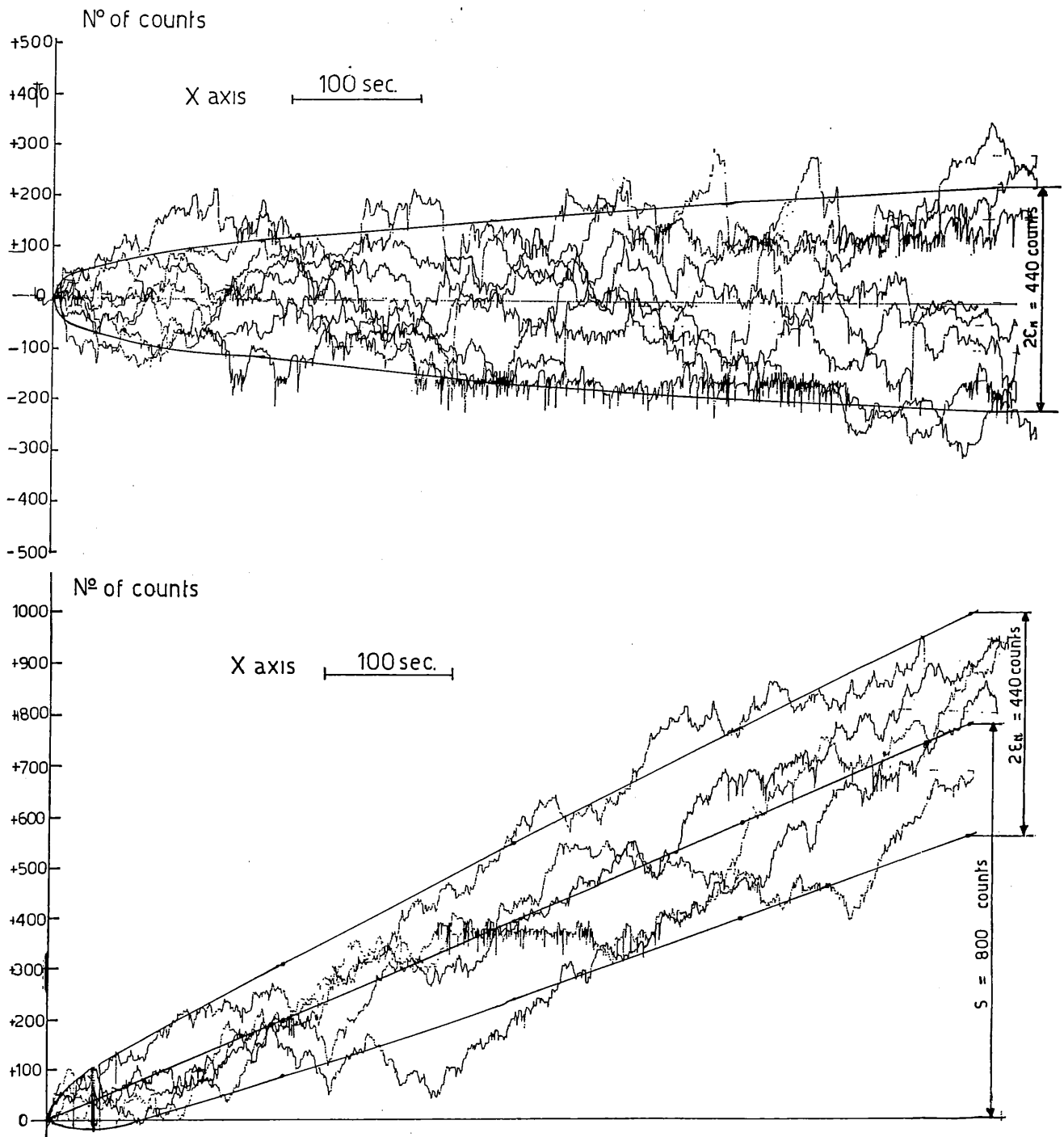


FIG. 6. Random walks of the counter reading and theoretical noise parabolas with no signal pulses (upper graph). Noise pulse rate  $\eta f_n = 33.5$  pulses/sec and integration time  $T = 12$  min. In the lower graph a signal with a pulse rate  $\eta f_s = 1.1$  photoelectrons/sec was added.

out signal pulses (upper graph), and in the presence of a very weak signal ( $\eta f_s = 1.1$  photoelectrons/sec) (lower graph), which can be detected after 12 min of integration with a signal-to-noise ratio of 3.6. The chopping frequency  $\nu_0$  was set at 125 cps. The bidirectional counter has both a digital reading, and an analog output for operation in connection with a strip chart recorder.

**ACKNOWLEDGMENTS**

The authors take pleasure in thanking Profs. G. Careri and V. Svelto for useful discussions and G. Lepre for careful design and construction of the electronic circuitry and assistance in the measurements.

**APPENDIX**

The notations<sup>1</sup> used in the text for the noise analysis of Sec. 3 are reported in the following table.

Function $f(t)$	Fourier transform $F(\omega)$
$\text{rect}(t/\tau) = \begin{cases} 1, &  t/\tau  < \frac{1}{2} \\ 0, &  t/\tau  > \frac{1}{2} \end{cases}$	$\tau \text{ sinc}(\omega\tau/2\pi) = \tau [\sin(\omega\tau/2\pi)]/(\omega\tau/2\pi)$
$\text{rep}_{\nu_0} u(t) = \sum_{n=-\infty}^{n=+\infty} u[t - (n/\nu_0)]$	$\nu_0 \text{ comb}_{\nu_0} U(\omega) = \nu_0 \sum_{n=-\infty}^{n=+\infty} U(2\pi n\nu_0) \delta(\omega - 2\pi n\nu_0)$
$u(t)$	$U(\omega)$